Diagnostic value of lung thallium-201 uptake in detecting high-risk coronary artery disease using cadmium-zinc-telluride camera system

Tetsushi SAITOH, Taishiro CHIKAMORI, Satoshi HIDA, Hirokazu TANAKA,

Yuko IGARASHI, Chie SHIBA, Kimihiko HIROSE, Tsuguhisa HATANO,

Akira YAMASHINA

Department of Cardiology, Tokyo Medical University

Abstract

Background : Stress lung thallium-201 uptake is a marker for high-risk coronary artery disease (CAD) when using a conventional Anger camera. To our knowledge, no other study has investigated whether stress lung thallium-201 uptake when using a cadmium-zinc-telluride (CZT) camera offers increased diagnostic value over standard myocardial perfusion analysis in detecting high-risk CAD as defined by the Duke CAD Prognostic Index.

Methods : One-hundred ninety-seven consecutive patients underwent stress thallium-201 SPECT followed by coronary angiography within 3 months. The cut-off point for high-risk CAD was 42 on the Duke CAD Prognostic Index. On reconstructed coronal tomographic images, regions of interest were placed over the left middle lung field and left ventricular myocardium. The ratio of lung-to-heart thallium-201 uptake after stress (stress L/H-ratio) was calculated as a fraction of thallium-201 counts per pixel in the lung divided by that in the myocardium.

Results : Examination of 86 patients with high-risk CAD revealed a summed difference score (SDS) of ≥ 10 and stress L/H-ratio of ≥ 0.33, with sensitivities of 67% and 76%, and specificities of 81% and 63%, respectively. Multivariate analysis revealed that the combination of age ≥ 70, SDS ≥ 10, and stress L/H-ratio ≥ 0.33 identified high-risk CAD (sensitivity, 78% ; specificity, 73% ; chi-square, 81) better than the combination of age and SDS only (sensitivity, 67% ; specificity, 81% ; chi-square, 66).

Conclusion : Stress L/H-ratio analysis with conventional perfusion analysis better identifies high-risk CAD on the Duke CAD Prognostic Index, even with the CZT camera.

Introduction

Myocardial perfusion imaging (MPI) by single-photon emission computed tomography (SPECT) is widely used in clinical practice not only for diagnosing the presence or absence of coronary artery disease (CAD), but also for evaluating disease severity[1]. A new-generation SPECT system incorporating semiconductor cadmium-zinc-telluride (CZT) detector technology has recently been developed. This new system provides superior image quality, reduced acquisition times, and lower radiotracer doses than the conventional Anger camera[2-5]. Lung thallium-201 uptake after stress is a well-known marker for severe and extensive CAD with the conventional Anger camera system[6-13]. To our knowledge, however, no study to date has investigated whether lung thallium-201 uptake with the new CZT camera offers increased diagnostic value over standard myocardial perfusion analysis in detecting high-risk CAD. Therefore, the purpose of this study was to retrospectively investi-

gate whether lung thallium-201 uptake with the CZT camera offers increased diagnostic value over standard myocardial perfusion analysis in detecting high-risk CAD as defined by the Duke CAD Prognostic Index.

Methods

Study Patients

A total of 197 consecutive patients (161 men and 36 women ; mean age 69±10 yr) were enrolled in the study between November 2011 and August 2014. All patients had either suspected or known CAD based on clinical symptoms, coronary risk profiles, electrocardiographic findings, or past medical history ; all patients also underwent stress thallium-201 SPECT using the new CZT camera system and coronary angiography within 3 months thereafter. Previous myocardial infarction had occurred in 44 of these patients. The exclusion criteria were as follows : acute myocardial infarction ; unstable angina ; acute heart failure within 1 month before the study ; previous coronary artery bypass grafting ; moderate or severe valvular heart disease ; hemodialysis ; chronic obstructive pulmonary disease ; and non-ischemic cardiomyopathy. Written informed consent for invasive coronary angiography was obtained from all participants. This retrospective study was approved by the Ethics Committee of Tokyo Medical University (No. 3438).

Stress myocardial perfusion imaging

The study protocol for stress MPI is shown in Fig. 1. Exercise MPI with thallium-201 was performed in 70 patients using a 1-day protocol. Symptom-limited, multi-step exercise using a bicycle ergometer was performed[14]. Thallium-201 (74 MBq) was given at 85% of the age-adjusted predicted maximum heart rate (target heart rate), or when chest pain, ST-segment depression ≥ 0.1 mV, or leg fatigue developed. Exercise was then continued for 1 min at the same exercise level. Immediately after this last exercise session, ECG-gated SPECT was acquired. Four hours later, thallium-201 ECG-gated SPECT at rest was also obtained. Adenosine tri-

phosphate (ATP) loading stress MPI was performed in 127 patients[15]. Cardioactive medications were withdrawn 24 hr before the SPECT study. Patients were also requested not to drink any beverage containing caffeine for at least 12 hr before the test. Adenosine triphosphate disodium (0.16 mg·kg^{-1}·min^{-1}) was given intravenously for 5 min followed by intravenous thallium-201 (74 MBq) 3 min later. Image acquisition was started immediately after stress application. Thallium-201 ECG-gated SPECT images at rest were acquired 4 hr later.

Data were acquired in a list mode using the CZT camera (Discovery NM530c ; GE Healthcare, Haifa, Israel)[16]. This SPECT system is equipped with a multiple-pinhole collimator and 19 stationary CZT detectors that simultaneously focus on the heart. The CZT pixels are 2.46 × 2.46 mm in size and each detector contains 32 × 32-pixel 5-mm-thick elements. The stationary array simultaneously acquires all the views necessary for tomographic reconstruction[17]. Image acquisition was performed in the supine and prone positions after stress for 5 min and 3 min, respectively, and in the supine position at rest for 10 min. For prone position imaging, the patients lie prone on the table while the detectors are rotated underneath it. Interpretation of the inferior wall was assisted by this prone position imaging, which can decrease the frequency of attenuation artifacts in the inferior wall[18].

A workstation (Xeleris ; GE Healthcare) incorporating a new dedicated iterative algorithm with integrated collimator geometric modeling was used for reconstruction of the SPECT images. This modeling involved maximum penalized likelihood iterative reconstruction to obtain perfusion images in the standard axes[19)20]. For both stress and rest image reconstruction, 70 iterations were used. A Butterworth filter (order 15 ; cut-off frequency, 0.28 cycles/cm) was applied to the reconstructed slices. When obtaining ECG-gated images, the R-R interval was divided into 8 equal portions by the R wave trigger. Each reconstructed short-axis thallium-201
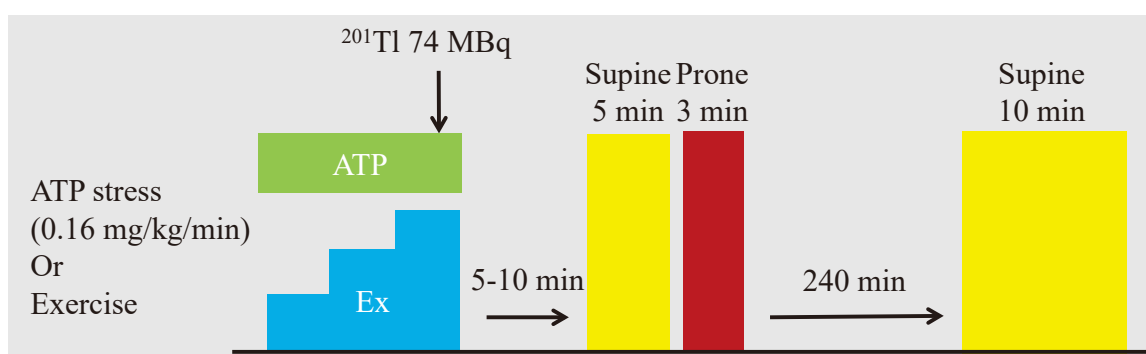
Fig. 1 Study protocol of stress myocardial perfusion imaging.
ATP : adenosine triphosphate

ECG-gated SPECT image was processed and left ventricular (LV) functional parameters (LV end-diastolic volume, LV end-systolic volume, and LV ejection fraction) automatically obtained using a quantitative gated SPECT program as described by Germano et al[21]. Of 197 patients, 191 (96%) showed sinus rhythm during image acquisition. No scatter or attenuation corrections were made.

In accordance with a previously reported method, each SPECT image was divided into 17 segments[22]. The radiopharmaceutical accumulation in the myocardium was visually evaluated by 2 cardiologists who were blinded to the clinical data. A 5-grade scale was used : 0, normal ; 1, slight reduction in uptake ; 2, moderate reduction in uptake ; 3, severe reduction in uptake ; or 4, absence of radioactive uptake. The sum of the scores for all the segments during exercise and at rest was termed the summed stress score (SSS) and summed rest score (SRS), respectively. The SSS minus the SRS was defined as the summed difference score (SDS)[23]. Disagreements in image interpretation were resolved by consensus. To adequately secure the position of the lung

using the CZT camera, a pilot study was performed to identify the location of the heart and lung by fusing images acquired from 10 patients who underwent both coronal imaging using the CZT camera and chest computed tomography (Fig. 2). These patients comprised 6 men and 4 women, and their mean age, height, body weight, and body mass index were 75 ± 10 years, 161.8 ± 8.0 cm, 58.4 ± 8.6 kg and 22.2 ± 1.9, respectively. The LV end-diastolic volume, LV end-systolic volume, and LV ejection fraction at stress using quantitative gated SPECT software were 69 ± 19 ml, 28 ± 15 ml, and $57 \pm 12\%$, respectively. The results showed that the left middle lung field was located along the upper right diagonal of the heart on the coronal image. The region of interest (ROI) was subsequently placed over the left middle lung field. Lung thallium-201 activity was measured by placing a 5.0×5.0-pixel ROI over the left middle lung field, while LV myocardium activity was measured by a ROI drawn around the entire LV myocardium (Fig. 3). The ratio of lung-to-heart thallium-201 uptake (L/H-ratio) after stress was calculated as a fraction of thallium-201 counts per pixel in the lung divided by that in
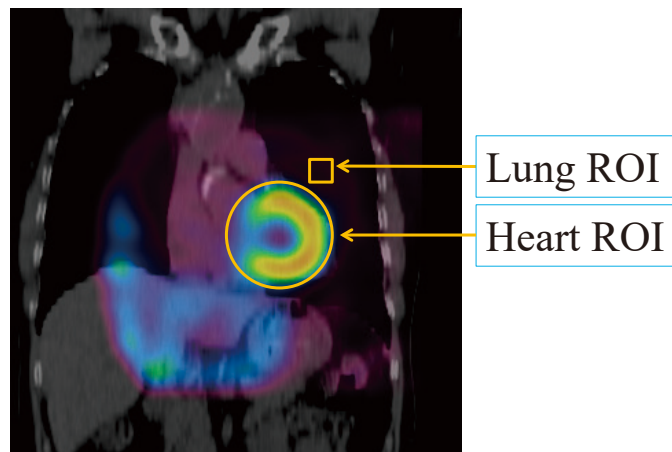
Fig. 2　To adequately secure position of lung using CZT camera, pilot study was conducted to identify location of heart and lung by fusing images acquired from 10 patients who underwent both coronal imaging using CZT camera and chest computed tomography. Lung ROI : regions of interest of lung. Heart ROI : regions of interest of heart.
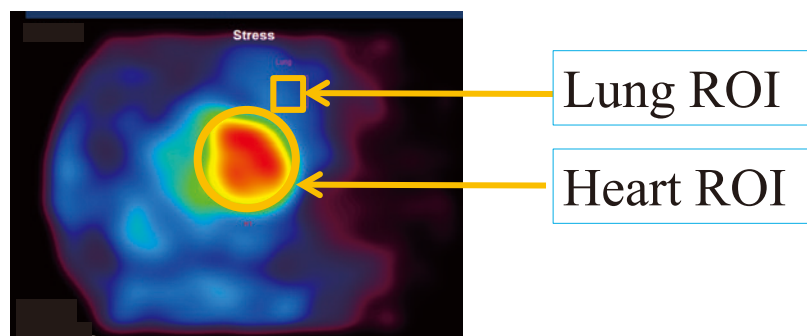
Fig. 3　On reconstructed coronal tomographic image, regions of interest were placed over left middle lung field and left ventricular myocardium. Ratio of lung-to-heart thallium-201 uptake after stress (stress L/H-ratio) was calculated as fraction of thallium-201 counts per pixel in lung divided by that in myocardium. Lung ROI : regions of interest of lung. Heart ROI : regions of interest of heart.

the myocardium.

Coronary angiography

Multidirectional coronary angiography was performed using the Judkins' method within 3 months of the scintigraphic study in all patients.　The degree of coronary artery stenosis was visually rated according to the criteria of the American Heart Association[24].　Significant stenosis was considered to be present when ≥ 75% narrowing of the diameter was observed.

The severity of CAD was assessed using the Duke Prognostic Index.　This index considers both the number of diseased vessels (1-, 2-, and 3-vessel disease, as well as left main trunk disease) and the involvement of the left anterior descending coronary artery, particularly in cases of proximal involvement and severe stenosis (i.e., ≥ 95%).　The index comprised 16 angiographic subsets that were assigned prognostic weights of from 0 to 100.　Severe CAD was defined as CAD with a prognostic weight of ≥ 42 on the CAD Prognostic Severity Index[25][26].

Statistical analysis

The results are expressed as the mean ± SD.　A Student's t-test was used to compare the means of continuous variables, and contingency tables were analyzed using the χ^2 test.　Receiver-operating characteristic (ROC) curves were analyzed to determine the optimal cut-offs for SSS, SDS, and stress L/H-ratio.　Sensitivity and specificity for each of these cut-offs were calculated using standard formulas.　Univariate analysis was conducted with the logistic regression method, while stepwise multivariate analysis was conducted with the multiple logistic regression method using statistically significant variables obtained from the univariate analysis.　Linear discriminant analysis was performed with stepwise variable selection with Wilks' lambda (the ratio of the within-groups sum of squares to the total sum of squares) to assess the potential to correctly identify high-risk CAD using independent variables on multivariate analysis.　A Bayes rule with equal prior probability was used for identification, and the results are presented as sensitivity, specificity, and accuracy.　A p value of < 0.05 was considered to represent a statistically significant difference.　The statistical computations were performed using SPSS 24 (IBM Corp., Armonk, NY, USA) and MedCalc 16.4.3 (MedCalc Software, Mariakerke, Belgium).

Results

Patient characteristics

The clinical characteristics of the patients, including medication at the time of the study, are summarized in Table 1.　All patients underwent coronary angiography : 1-vessel CAD was found in 54 patients, 2-vessel CAD in 45, 3-vessel CAG in 43, and insignificant lesions in the remaining 55.　Fourteen patients, 1 with 2-vessel CAD and 13 with 3-vessel CAD, also had significant stenosis in the left main trunk.　The average Duke Prognostic CAD Index score was 34 ± 24 (0 to 82).　Among the 197 patients, 86 (44%) had high-risk CAD as defined by the previous definition[25].　Eighty-six patients with high-risk CAD were older (72 ± 8 yr vs. 67 ± 10 yr ; p = 0.001) and had a higher prevalence of hypertension (88% vs. 77% ; p = 0.047) and diabetes mellitus (51% vs. 31% ; p = 0.003) than the 111 without high-risk CAD, while the prevalence of the remaining coronary risk factors was similar.

Myocardial perfusion imaging

In patients with high-risk CAD, the SSS (19.3 ± 9.0 vs. 11.7 ± 7.7 ; p < 0.0001) and SDS (12.2 ± 6.6 vs. 5.6 ± 5.4 ; p < 0.0001) were greater than those in patients without high-risk CAD, whereas the SRS, LV end-diastolic volume, end-systolic volume, and ejection fraction after stress and at rest were similar (Table 1).　The stress L/H-ratio (0.37 ± 0.06 vs. 0.31 ± 0.06 ; p < 0.0001) was significantly greater in patients with high-risk CAD than in those without.

Univariate analysis for detection of high-risk CAD

An ROC curve analysis was performed to detect high-risk CAD using myocardial perfusion analysis.　The cut-off points for high-risk CAD were ≥ 13 for SSS, ≥ 10 for SDS, and ≥ 0.33 for stress L/H-ratio (Fig. 4).　In addition, the optimal cut-off points for the stress L/H-ratio to detect high-risk CAD were the same for the 70 patients who underwent exercise stress and the 127 patients who were evaluated with ATP loading.　The respective sensitivities, specificities, and accuracies in the detection of high-risk CAD were 78%, 66% and 71% with SSS, 67%, 81%, and 75% with SDS, and 76%, 63% and 69% with the stress L/H-ratio, respectively (Table 2).

Multivariate analysis for detection of high-risk CAD

Logistic regression analysis was performed to detect high-risk CAD by entering 6 variables that were statistically significant on univariate analysis (Table 3).　This revealed that age, SDS, and stress L/H-ratio were independent variables.　In the multivariate analysis, age ≥ 70 yr and SDS ≥ 10 were significantly associated with high-risk CAD.　Linear discriminant analysis using age and myocardial perfusion yielded 67% sensitivity, 81% specificity, and 75% accuracy (global χ^2 = 66 ; Fig. 5).　Discriminant analysis using age, myocardial perfusion, and the stress L/H-ratio, which were statistically significant on multivariate analysis, was repeated.　The results showed that the combination of age ≥ 70, SDS ≥ 10, and stress L/H-ratio ≥ 0.33 best identified high-risk CAD, with a sensitivity of 78%, specificity of 73%, and accuracy of 75% (global χ^2 = 81 ; Fig. 5).

Table 1   Comparison of clinical characteristics between patients with and without high-risk CAD

	High-risk CAD (+) (n = 86)	High-risk CAD (−) (n = 111)	p-value
Age (years)	72 ± 8	67 ± 10	0.001
Men (%)	73 (85)	88 (79)	NS
Body mass index	24.6 ± 3.3	24.3 ± 4.3	NS
Hypertension (%)	76 (88)	86 (77)	0.047
Dyslipidemia (%)	73 (85)	82 (74)	NS
Diabetes mellitus (%)	44 (51)	34 (31)	0.003
Smoking (%)	56 (55)	69 (62)	NS
Prior MI (%)	18 (21)	26 (23)	NS
Prior PCI (%)	26 (30)	46 (41)	NS
Prior CABG	0	0	NS
AF (%)	4 (5)	2 (2)	NS
Myocardial perfusion			
SSS	19.3 ± 9.0	11.7 ± 7.7	< 0.0001
SRS	7.1 ± 7.1	6.1 ± 6.9	NS
SDS	12.2 ± 6.6	5.6 ± 5.4	< 0.0001
LV function after stress			
EDV (ml)	81 ± 32	82 ± 28	NS
ESV (ml)	37 ± 27	36 ± 23	NS
EF (%)	58 ± 13	59 ± 12	NS
LV function at rest			
EDV (ml)	74 ± 30	80 ± 30	NS
ESV (ml)	35 ± 26	36 ± 25	NS
EF (%)	59 ± 13	59 ± 12	NS
stress L/H-ratio	0.37 ± 0.06	0.31 ± 0.06	< 0.0001

Data given as mean ± SD or n (%)

MI : myocardial infarction ; PCI : percutaneous coronary intervention ; CABG : coronary artery bypass grafting ; AF : atrial fibrillation ; CAD : coronary artery disease ; SSS : summed stress score ; SRS : summed rest score ; SDS : summed difference score ; LV : left ventricular ; EDV : end-diastolic volume ; ESV : end-systolic volume ; EF : ejection fraction ; stress L/H-ratio : ratio of lung-to-heart thallium-201 uptake after stress
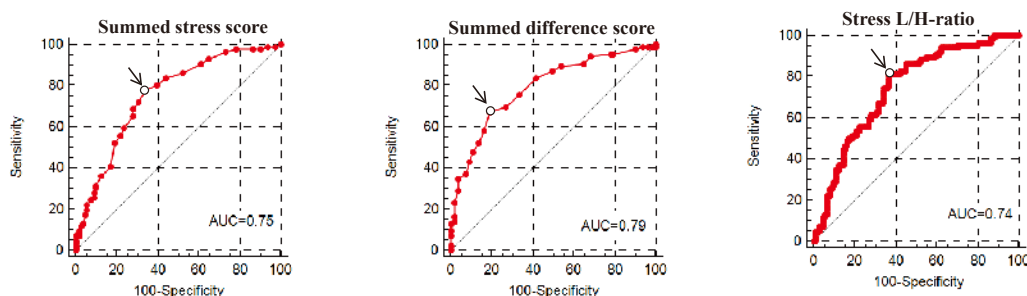
Fig. 4   (A) Cut-off points for perfusion parameters and stress L/H-ratio to detect high-risk coronary artery disease (CAD).   Cut-off points for high-risk CAD were defined as summed stress score of ≥ 13 (area under curve [AUC = 0.75]), summed difference score of ≥ 10 (AUC = 0.79), and stress L/H-ratio of ≥ 0.33 (AUC = 0.71).   Stress L/H-ratio : ratio of lung-to-heart thallium-201 uptake after stress.

Discussion

To the best of our knowledge, this is the first study to investigate whether increased stress lung thallium-201 uptake using the new CZT camera system offers increased diagnostic value over conventional MPI analy-

sis in the detection of high-risk CAD.   Extensive and severe myocardial perfusion abnormalities as represented by summed scores are well-established scintigraphic markers for high-risk CAD[27)28)].   Indeed, an SDS of ≥ 10 and SSS of ≥ 13 were significantly associated with high-risk CAD in the present study.   Multivariate analy-

Table 2　Diagnostic value of each scintigraphic parameter for high-risk CAD

	Sensitivity (%)	Specificity (%)	Accuracy (%)
SSS ≥ 13	78	66	77
SDS ≥ 10	67	81	75
stress L/H-ratio ≥ 0.33	76	63	69

CAD : coronary artery disease ; SSS : summed stress score ; SDS : summed difference score ; stress L/H-ratio : ratio of lung-to-heart thallium-201 uptake after stress

Table 3　Univariate and multivariate analysis for detection of high-risk CAD

Variable	Univariate Analysis		Multivariate Analysis	
	OR (95% CI)	*p*-value	OR (95% CI)	*p*-value
Age ≥ 70	2.9 (1.6-5.3)	< 0.0001	4.1 (1.9-8.8)	0.003
Male	0.7 (0.3-1.4)	NS		
Hypertension	2.2 (1.0-4.9)	0.047	1.7 (0.6-4.5)	0.32
Dyslipidemia	2.0 (1.0-4.1)	NS		
Diabetic mellitus	2.4 (1.3-4.3)	0.003	1.8 (0.9-3.6)	0.12
Smoking	1.1 (0.6-2.0)	NS		
Prior PCI	0.6 (0.3-1.1)	NS		
SSS ≥ 13	6.8 (3.6-12.9)	< 0.0001	2.1 (0.8-5.5)	0.11
SDS ≥ 10	8.9 (4.6-17.1)	< 0.0001	4.2 (1.6-10.7)	0.0027
stress L/H-ratio ≥ 0.33	5.2 (2.8-9.9)	< 0.0001	3.7 (1.8-7.8)	0.0005

PCI : percutaneous coronary intervention ; SSS : summed stress score ; SDS : summed difference score ; stress L/H-ratio : ratio of lung-to-heart thallium-201 uptake after stress
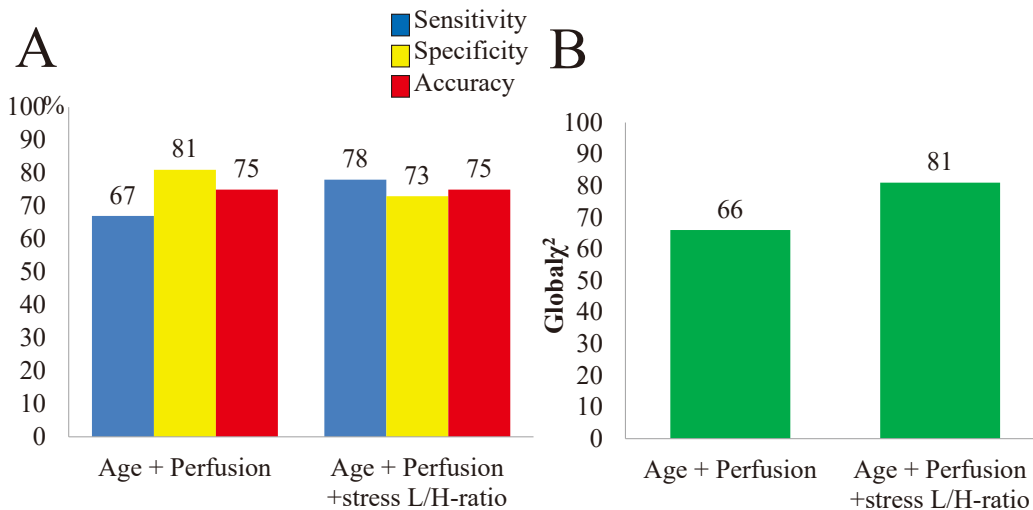
Fig. 5　(A) Comparison of diagnostic value of addition of stress L/H-ratio in detection of high-risk CAD.　Stress L/H-ratio : ratio of lung-to-heart thallium-201 uptake after stress.
(B) Improved diagnostic value with addition of stress L/H ratio to age + perfusion analysis in detection of high-risk CAD.

sis showed that the combination of the stress L/H-ratio, age, and myocardial perfusion abnormalities best identified patients with high-risk CAD, with a higher sensitivity of 78% and a lower specificity of 73% than age and perfusion alone, which showed 67% sensitivity and 81% specificity.　Stress lung thallium-201 uptake on myocardial SPECT was observed to improve sensitivity and diagnostic value considerably (global χ^2 : 81 vs. 66) over

clinical and perfusion variables without lung thallium-201 uptake in the detection of high-risk CAD. While previous studies using an Anger camera reported the usefulness of increased lung thallium-201 uptake on stress MPI in detecting extensive CAD[6-8)11)], the present study showed that stress lung thallium-201 uptake yielded increased diagnostic value with the new CZT camera system.

Many previous studies using Anger cameras have reported the diagnostic and prognostic value of increased lung thallium-201 uptake on MPI in patients with CAD[6-13)].   Most of these studies evaluated planar images in which adequate placement of an ROI in the myocardium and lung was not difficult.   By contrast, heart imaging is obtained and created using a plurality of pinhole collimators focused on the heart and 19 fixed CZT detectors in the CZT camera.   Therefore, unlike with an Anger camera, it is difficult to create a planar image with a CZT camera.   For this reason, here, a new method was used in which the coronal image was reconstructed using the CZT camera.   Prior to the start of the current study, the location of the heart and the left middle lung field was assessed with the CZT camera using fusion imaging with myocardial SPECT and chest computed tomography.

In previous studies using Anger cameras, the stress L/H-ratio cut-off point was defined as 0.50[8)29-32)].   In the present study, the optimal cut-off point for high-risk CAD was defined as 0.33 using the CZT camera. Although lung thallium-201 uptake tended to be lower with pharmacological stress than with exercise stress in previous studies[30)33)34)], the cut-off point for high-risk CAD with pharmacological stress was equivalent to that with exercise stress in the present study.   The difference in cut-off points between this and previous studies was, however, unsurprising as different methods were used.

Several underlying mechanisms for increased lung thallium-201 uptake after stress have been proposed.   In exercise stress MPI, the mechanisms of abnormal thallium-201 uptake were believed to be due to elevated pulmonary capillary wedge pressure secondary to stress-induced ischemia[6)7)35)].   In pharmacologic stress MPI, coronary steal phenomenon due to pharmacological vasodilator action results in ischemic LV dysfunction. Thus, rising LV filling pressure and pulmonary capillary pressure caused abnormal lung thallium-201 uptake[33)36)].

Traditionally, left main, 3-vessel, or multi-vessel CAD is regarded as a high-risk CAD subset.   However, 1-vessel CAD with severe stenosis of the proximal left anterior descending artery is not considered to be a high-risk group according to conventional classification.   To overcome this, the Duke Prognostic Index was developed, and this was the index applied in the current study. Based on this index, most patients in the high-risk group had significant stenosis of the left main trunk or severe stenosis of the proximal left anterior descending artery, regardless of the number of diseased vessels.   This approach is relevant to clinical practice, where decision-making that leads to better patient prognosis—rather than simply diagnosing coronary artery disease—is the most important.

In general, MPI is often unsuccessful in detecting high-risk CAD such as when it is multi-vessel because scintigraphic interpretation relies on spatially relative perfusion defect analysis.   Thus, uniform global hypoperfusion due to a reduction in the balance of myocardial blood flow may result in a decrease in summed scores, which may then lead to underestimation of the potential for high-risk CAD and decreased sensitivity.   In contrast to MPI, however, stress lung thallium-201 uptake analysis based on CZT SPECT is independent of the shortcomings of relative perfusion defect analysis, which allows it to reveal the absolute values of stress lung thallum-201 uptake.   Therefore, the addition of lung thallium-201 uptake analysis further increases sensitivity in identifying groups at high-risk of CAD.   However, patients with LV dysfunction such as old myocardial infarction may have an increased L/H ratio and care must therefore be taken in such cases.

Study Limitations

In the present study, the degree of coronary artery stenosis was visually rated according to the criteria of the American Heart Association[23)].   Therefore, it was difficult to determine whether the lesion was true or false in cases of an intermediate coronary lesion.   This indicates that intermediate lesions should be evaluated using fractional flow reserve[37)].

Another limitation is that the current study was performed retrospectively at a single institution.   Therefore, further prospective study including multiple centers is necessary.

Conclusion

Including an analysis of the stress L/H-ratio in conventional perfusion analysis may help better identify patients at high risk of CAD, even with the CZT camera system.

Conflict of Interest : The authors declare no conflict of interest.

References

1) Klocke FJ, Baird MG, Lorell BH, Bateman TM, Messer JV, Berman DS, O'Gara PT, Carabello BA, Russell RO Jr, Cerqueira MD, St John Sutton MG, DeMaria AN, Udelson JE, Kennedy JW, Verani MS, Williams KA, Antman EM, Smith SC Jr, Alpert JS, Gregoratos G, Anderson JL, Hiratzka LF, Faxon DP,

Hunt SA, Fuster V, Jacobs AK, Gibbons RJ, Russell RO : ACC/AHA/ASNC Guidelines for the clinical use of cardiac radionuclide imaging—executive summary. J Am Coll Cardiol **42** : 1318-1333, 2003

2) Herzog BA, Buechel RR, Katz R, Brueckner M, Husmann L, Burger IA, Pazhenkottil AP, Valenta I, Gaemperli O, Treyer V, Kaufmann PA : Nuclear myocardial perfusion imaging with a cadmium-zinc-telluride detector technique : optimized protocol for scan time reduction. J Nucl Med **51** : 46-51, 2010

3) Duvall WL, Croft LB, Godiwala T, Ginsberg E, George T, Henzlova MJ : Reduced isotope dose with rapid SPECT MPI imaging : initial experience with a CZT SPECT camera. J Nucl Cardiol **17** : 1009-1014, 2010

4) Songy B, Lussato D, Guernou M, Queneau M, Geronazzo R : Comparison of myocardial perfusion imaging using thallium-201 between a new cadmium-zinc-telluride cardiac camera and a conventional SPECT camera. Clin Nucl Med **36** : 776-780, 2011

5) Tanaka H, Chikamori T, Hida S, Uchida K, Igarashi Y, Yokoyama T, Takahashi M, Shiba C, Yoshimura M, Tokuuye K, Yamashina A : Comparison of myocardial perfusion imaging between the new high-speed gamma camera and the standard anger camera. Circ J **77** : 1009-1017, 2013

6) Bingham JB, McKusick KA, Strauss HW, Boucher CA, Pohost GM : Influence of coronary artery disease on pulmonary uptake of thallium-201. Am J Cardiol **46** : 821-826, 1980

7) Boucher CA, Zir LM, Beller GA, Okada RD, McKusick KA, Strauss HW, Pohost GM : Increased lung uptake of thallium-201 during exercise myocardial imaging : clinical, hemodynamic and angiographic implications in patients with coronary artery disease. Am J Cardiol **46** : 189-196, 1980

8) Kushner FG, Okada RD, Kirshenbaum HD, Boucher CA, Strauss HW, Pohost GM : Lung thallium-201 uptake after stress testing in patients with coronary artery disease. Circulation **63** : 341-347, 1981

9) Gibson RS, Watson DD, Carabello BA, Holt ND, Beller GA : Clinical implications of increased lung uptake of thallium-201 during exercise scintigraphy 2 weeks after myocardial infarction. Am J Cardiol **49** : 1586-1593, 1982

10) Okada RD, Dai YH, Boucher CA, Pohost GM : Significance of increased lung thallium-201 activity on serial cardiac images after dipyridamole treatment in coronary heart disease. Am J Cardiol **53** : 470-475, 1984

11) Liu P, Kiess M, Okada RD, Strauss HW, Block PC, Pohost GM, Boucher CA : Increased thallium lung uptake after exercise in isolated left anterior descending coronary artery disease. Am J Cardiol **13** : 1469-1473, 1985

12) Gill JB, Ruddy TD, Newell JB, Finkelstein DM, Strauss HW, Boucher CA : Prognostic importance of thallium uptake by the lungs during exercise in coronary artery disease. N Engl J Med **317** : 1486-1489, 1987

13) Jain D, Thompson B, Wackers FJ, Zaret BL : Relevance of increased lung thallium uptake on stress imaging in patients with unstable angina and non-Q wave myocardial infarction : results of the Thrombolysis in Myocardial Infarction (TIMI)-IIIB Study. J Am Coll Cardiol **30** : 421-429, 1997

14) Tanaka H, Chikamori T, Tanaka N, Hida S, Igarashi Y, Yamashita J, Ogawa M, Shiba C, Usui Y, Yamashina A : Diagnostic performance of a novel cadmium-zinc-telluride gamma camera system assessed using fractional flow reserve. Circ J **78** : 2727-2734, 2014

15) Hida S, Chikamori T, Tanaka H, Igarashi Y, Shiba C, Hatano T, Usui Y, Yamashina A : Postischemic myocardial stunning is superior to transient ischemic dilation for detecting multivessel coronary artery disease. Circ J **76** : 430-438, 2012

16) Bocher M, Blevis IM, Tsukerman L, Shrem Y, Kovalski G, Volokh L : A fast cardiac gamma camera with dynamic SPECT capabilities : design, system validation and future potential. Eur J Nucl Med Mol Imaging **37** : 1887-1902, 2010

17) Buechel RR, Herzog BA, Husmann L, Burger IA, Pazhenkottil AP, Treyer V, Valenta I, von Schulthess P, Nkoulou R, Wyss CA, Kaufmann PA : Ultrafast nuclear myocardial perfusion imaging on a new gamma camera with semiconductor detector technique : first clinical validation. Eur J Nucl Med Mol Imaging **37** : 773-778, 2010

18) Goto K, Takebayashi H, Kihara Y, Yamane H, Hagikura A, Morimoto Y, Kikuta Y, Sato K, Taniguchi M, Hiramatsu S, Haruta S : Impact of combined supine and prone myocardial perfusion imaging using an ultrafast cardiac gamma camera for detection of inferolateral coronary artery disease. Int J Cardiol **174** : 313-317, 2014

19) Esteves FP, Raggi P, Folks RD, Keidar Z, Askew JW, Rispler S, O'Connor MK, Verdes L, Garcia EV : Novel solid-state-detector dedicated cardiac camera for fast myocardial perfusion imaging : multicenter comparison with standard dual detector cameras. J Nucl Cardiol **16** : 927-934, 2009

20) Hebert T, Leahy R : A generalized EM algorithm for 3-D Bayesian reconstruction from Poisson data using Gibbs priors. IEEE Trans Med Imaging **8** : 194-202, 1989

21) Germano G, Kiat H, Kavanagh PB, Moriel M, Mazzanti M, Su HT, Van Train KF, Berman DS : Automatic quantification of ejection fraction from gated myocardial perfusion SPECT. J Nucl Med **36** : 2138-2147, 1995

22) Cerqueira MD, Weissman NJ, Dilsizian V, Jacobs AK, Kaul S, Laskey WK, Pennell DJ, Rumberger JA, Ryan T, Verani MS : Standardized myocardial seg-

mentation and nomenclature for tomographic imaging of the heart. A statement for healthcare professionals from the Cardiac Imaging Committee of the Council on Clinical Cardiology of the American Heart Association. Int J Cardiovasc Imaging **18** : 539-542, 2002

23) Berman DS, Abidov A, Kang X, Hayes SW, Friedman JD, Sciammarella MG, Cohen I, Gerlach J, Waechter PB, Germano G, Hachamovitch R : Prognostic validation of a 17-segment score derived from a 20-segment score for myocardial perfusion SPECT interpretation. J Nucl Cardiol **11** : 414-423, 2004

24) Austen WG, Edwards JE, Frye RL, Gensini GG, Gott VL, Griffith LS, McGoon DC, Murphy ML, Roe BB : A reporting system on patients evaluated for coronary artery disease. Report of the Ad Hoc Committee for Grading of Coronary Artery Disease, Council on Cardiovascular Surgery, American Heart Association. Circulation **51** : 5-40, 1975

25) Mark DB NelsonCL, CalifT RM, Harrell FE, Jr, Lee KL, Jones RH, Fortin DF, Stack RS, Glower DD, Smith LR, DeLong ER, Smith PK, Reves JG, Jollis JG, Tcheng JE, Muhlbaier JH, Lowe JE, Phillips HR, Pryor DB : Continuing evolution of therapy for coronary artery disease. Initial results from the era of coronary angioplasty. Circulation **89** : 2015-2025, 1994

26) Hida S, Chikamori T, Tanaka H, Igarashi Y, Shiba C, Hatano T, Usui Y, Yamashina A : Sex-specific approach to gated SPECT volumetric analysis after stress and at rest to detect high-risk coronary artery disease. Nucl Med Commun **31** : 800-806, 2010

27) McLaughlin MG, Danias PG : Transient ischemic dilation : a powerful diagnostic and prognostic finding of stress myocardial perfusion imaging. J Nucl Cardiol **9** : 663-667, 2002

28) Marcassa C, Galli M, Baroffio C, Campini R, Giannuzzi P : Transient left ventricular dilation at quantitative stress-rest sestamibi tomography : clinical, electrocardiographic, and angiographic correlates. J Nucl Cardiol **6** : 397-405, 1999

29) Chae SC, Heo J, Iskandrian AS, Wasserleben V, Cave V : Identification of extensive coronary artery disease in women by exercise single-photon emission computed tomographic (SPECT) thallium imaging. J Am Coll Cardiol **21** : 1305-1311, 1993

30) Villanueva FS, Kaul S, Smith WH, Watson DD, Varma SK, Beller GA : Prevalence and correlates of increased lung/heart ratio of thallium-201 during dipyridamole stress imaging for suspected coronary artery disease. Am J Cardiol **66** : 1324-1328, 1990

31) Homma S, Kaul S, Boucher CA : Correlates of lung/heart ratio of thallium-201 in coronary artery disease. J Nucl Med **28** : 1531-1535, 1987

32) Hansen CL, Sangrigoli R, Nkadi E, Kramer M : Comparison of pulmonary uptake with transient cavity dilation after exercise thallium-201 perfusion imaging. J Am Coll Cardiol **33** : 1323-1327, 1999

33) Nishimura S, Mahmarian JJ, Verani MS : Significance of increased lung thallium uptake during adenosine thallium-201 scintigraphy. J Nucl Med **33** : 1600-1607, 1992

34) Iskandrian AS, Heo J, Nguyen T, Lyons E, Paugh E : Left ventricular dilatation and pulmonary thallium uptake after single-photon emission computer tomography using thallium-201 during adenosine-induced coronary hyperemia. Am J Cardiol **66** : 807-811, 1990

35) Berman DS, Kiat H, Friedman JD, Wang FP, van Train K, Matzer L, Maddahi J, Germano G : Separate acquisition rest thallium-201/stress technetium-99m sestamibi dual-isotope myocardial perfusion single-photon emission computed tomography : a clinical validation study. J Am Coll Cardiol **22** : 1455-1464, 1993

36) Beller GA, Holzgrefe HH, Watson DD : Intrinsic washout rates of thallium-201 in normal and ischemic myocardium after dipyridamole-induced vasodilation. Circulation **71** : 378-386, 1985

37) Pijls NH : Fractional flow reserve to guide coronary revascularization. Circ J **77** : 561-569, 2013

テルル化亜鉛カドミウム半導体カメラを用いた
重症冠動脈疾患検出における肺タリウム–201 集積の診断的価値

齋 藤 哲 史　　　　近 森 大志郎　　　　肥 田　　敏
五十嵐 祐 子　　　　柴　　千 恵　　　　廣 瀬 公 彦
波多野 嗣 久　　　　山 科　　章

東京医科大学病院循環器内科学分野

【要旨】　従来の Anger 型 camera では thallium-201（Tl-201）を用いた心筋 SPECT での負荷時像肺・心臓集積比（stress L/H-ratio）亢進は高リスク冠動脈疾患（CAD）の指標として知られているが、cadmium zinc telluride（CZT）camera を用いた検討はない。【方法】CZT camera（Discovery NM530c）を用いて負荷 Tl-201 心筋 SPECT を行い、3 ヵ月以内に冠動脈造影を実施した連続 197 症例を対象とした。高リスク CAD は Duke CAD Prognostic Index を用いて 42 以上とした。冠状断撮影像を再構成し、関心領域を左中肺野と左心室とした。stress L/ H-ratio は Tl-201 の肺のピクセル当たりのカウントを心筋カウントで除して算出した。【結果】高リスク CAD 患者 86 例の検出能は summed difference score（SDS）≧ 10、stress L/H-ratio ≧ 0.33 がそれぞれ 67%、76%、特異度 81%、63% であった。多変量解析では年齢≧ 70、SDS ≧ 10 の組み合わせ（感度 67%、特異度 81%、global χ^2 = 66）より、年齢 ≧ 70、SDS ≧ 10、stress L/ H-ratio ≧ 0.33 の組み合わせが最も検出能に優れていた（感度 78%、特異度 73%、global χ^2 = 81）。【結論】CZT camera においても、心筋血流評価に stress L/H-ratio を追加することで高リスク CAD の診断精度が向上する可能性が示唆された。

〈キーワード〉冠動脈疾患、SPECT、テルル化亜鉛カドミウム半導体カメラ、肺タリウム-201 集積